Structural Monitoring and Maintenance, *Vol. 12, No. 1 (2025) 21-32*
https://doi.org/10.12989/smm.2025.12.1.021

Influence of rate-dependent properties of material on the spatial effects of seismic motion of bridge

Min Li*[1] and Liwei Shi[2a]

[1]*School of Marine and Civil Engineering, Dalian Ocean University, Dalian, 116023, China*
[2]*Beijing uni-construction group CO., LTD. Beijing, 100000, China*

(*Received August 12, 2024, Revised November 2, 2024, Accepted November 7, 2024*)

Abstract. Based on the finite element analysis software ABAQUS, a model of a reinforced concrete bridge is built. Using the time-history analysis method, the effects of the material strain rate on the spatial seismic response of the bridge are studied. The displacement time-history curves of the pier top and the shear force time-history curves of the pier base are plotted, and the dynamic responses of the bridge under consistent excitation and multi-support excitation are compared. The results indicate that when only the effects of material strain rate are considered, the displacement of the pier top is reduced and the shear force of the pier base is increased. When only the spatial effects of earthquake motion are considered, both the displacement value of the pier top and the shear force of the pier base are amplified. However, the strain rate effects of materials weaken the impact of seismic spatial effects on the pier displacement of the bridge to a certain degree.

Keywords: consistent excitation; multi-support excitation; seismic performance of bridge; strain rate

1. Introduction

The seismic performances of bridges are influenced by various factors, including the strain rate of materials and the spatial variability of earthquakes. Previous studies by Suaris (1983), Fu (1991), Takeda (1974), Fujikake (2000), Nie (2017), Chen (2018) and Kim (2020) have demonstrated that the behavior of solid materials under fast loading is different from that under slow loading. It is generally acknowledged that the primary factor causing significant differences in the mechanical properties of solid materials under dynamic loading compared to static loading is the strain rate sensitivity of material. Both steel and concrete are rate-sensitive materials, and they exhibit different mechanical and deformation properties at different strain rates. Currently, research on the impact of strain rate of materials on structures mainly focuses on explosion scenarios. Wei (2007), Chen (2008), Liu (2003), Yan (2005), Nam (2016) and Gang (2017) have conducted some studies in this field, and Pang (2009) studied the stress and deformation characteristics of concrete bridges under explosive loads. However, there is limited research about the effects of material's strain rate on bridge structures subjected to earthquake loading.

*Corresponding author, Associate Professor, E-mail: cnlm225@126.com
[a]MA., E-mail: 352844557@qq.com

 ISSN: 2288-6605 (Print), 2288-6613 (Online)

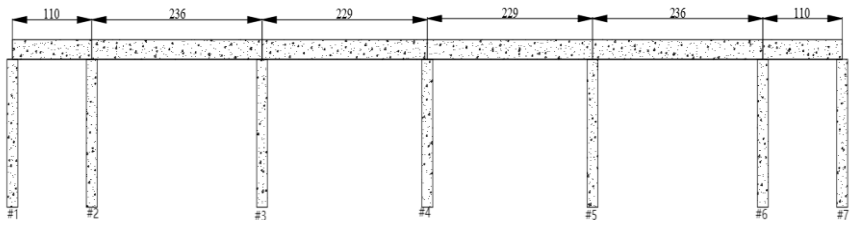

Fig. 1 Dimensions of the bridge(m)

The spatial variability of seismic motion is another crucial factor in seismic response analysis. For small or medium-length bridges, it is reasonable to assume that all support points experience uniform excitation. For bridges with large spans or lengths, it is necessary to consider the differences in seismic loading arising from varying geological conditions or differences in the arrival time of seismic waves (i.e., traveling wave effect), necessitating the use of multi-support excitation methods.

There are only a few studies on the influence of material's strain rate on the bridge structure under the earthquake action. Liu (2019) studied the dynamic response of an offshore bridge, considering the impact of the material's strain rate. In Liu's (2014) study,the strain rate effect of the material was considered in the analysis of large span single tower cable-stayed bridge. In the study of Li (2010), the seismic response and damage analysis of a continuous rigid structure bridge under traveling wave excitation and consistent excitation were conducted, using the elastoplastic damage model related to strain rate.The simulation results showed that the displacement time-history response was not sensitive to the strain rate effect, whereas the tensile and compressive damage distribution and evolution were sensitive, and the traveling wave effect influenced the displacement time-history response and damage distribution of the long, high pier, with a complex influence pattern.

In this paper, based on the finite element analysis software ABAQUS, a model of bridge is built. The effects of the material strain rate on the spatial seismic response of the bridge under different working conditions are studied.

2. Model of the bridge

A bridge from practical project has been selected, this standard compiled by GTJ (2015) is referenced in the design of the bridge structure. The bridge is a continuous beam bridge with equal cross-section. It is symmetrical with six spans and seven piers. The total length of the bridge is 1150 meters, and the height of each pier is 20 meters, the bridge is shown in Fig. 1. The main beam is connected to the piers using high damping rubber bearings. The seismic fortification intensity is 8 degrees, and the design service life is 120 years. The main beam is made of steel with a yield strength is 345 Mpa. The concrete used in the piers has a cubic compressive strength of 50 Mpa, and the yield strength of longitudinal reinforcement in pier is 335 Mpa. The diameter of the reinforcement is 40 mm, and the thickness of the concrete protective layer is 60 mm. The cross-sectional dimensions of the main beam of the bridge are shown in Fig. 2, and the cross-sectional dimensions of the piers are shown in Fig. 3.

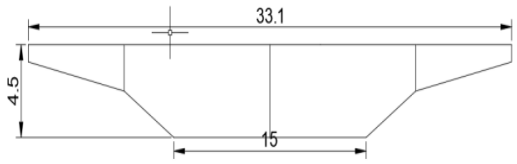

Fig. 2 The cross-sectional dimensions of beam (m)

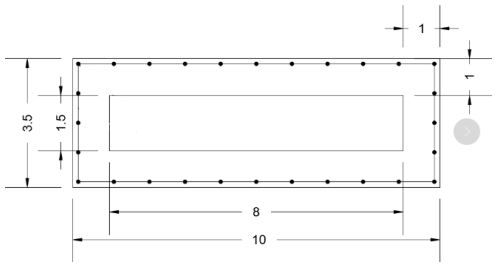

Fig. 3 The cross-sectional dimensions of pier (m)

Table 1 Q345 Material Parameters

Material	Strain rate (1/sec)	Yield strength (MPa)
Q345	1×10^{-4}	374
	1×10^{-3}	374
	5×10^{2}	536

A three-dimensional finite element model of the bridge is established, utilizing the ABAQUS program. The concrete piers employ C3D8R reduced integration elements, the steel beams utilize B31 beam elements, and the reinforcing steel bars adopt T3D2 truss elements. The bearings are simulated using SPRING2 elements. The main beam and bearings are connected through Tie constraints, and similarly, the piers and bearings are also constrained through Tie connections. The concrete employs the damage-plastic model provided by the software, while the springs utilize the elastic model. Both the reinforcing steel and the steel beams adopt the ideal elastic-plastic model, and the elastic modulus of steel are not influenced by the strain rate variations.

The material parameters for Q345 steel are based on the test results of Q345 steel under dynamic loading conducted by Yu (2011), and the values of material parameters are shown in Table 1.

The strain rate effect for HRB335 reinforcing steel is characterized the dynamic enhancement factor from the dynamic constitutive model of steel proposed by Li (2011).

$$\frac{f_{yd}}{f_{ys}} = 1.0 + c_f \lg \frac{\dot{\varepsilon}_s}{\dot{\varepsilon}_{s0}} \tag{1}$$

$$c_f = 0.1709 - 3.289 \times 10^{-4} f_{ys} \tag{2}$$

here, f_{ys}、f_{yd} represent the quasi-static and dynamic yield strengths of steel, respectively. $\dot{\varepsilon}_s$ is

the strain rate of steel, and $\dot{\varepsilon}_{s0}$ denotes the quasi-static strain rate of steel, which is typically $2.5 \times 10^{-4} s^{-1}$.

The strain rate effect on concrete compressive strength adopts the dynamic enhancement factor from the dynamic constitutive model of concrete proposed by Li (2011).

$$f_{cd} = f_c DIF\left(\dot{\varepsilon}\ ,\ f_{cu}\right) \tag{3}$$

$$DIF = 1.0 + 0.0314lg\left(\frac{\dot{\varepsilon_c}}{\dot{\varepsilon_{c0}}}\right) \tag{4}$$

here, f_{cd} and f_c represent the dynamic and quasi-static compressive strength of concrete, respectively. Meanwhile $\dot{\varepsilon}_c$ and $\dot{\varepsilon}_{c0}$ denote the strain rate and quasi-static strain rate of concrete, respectively. $\dot{\varepsilon}_{c0} = 1.0 \times 10^{-5} s^{-1}$ is chosen here.

The strain rate effect on concrete tensile strength adopts the dynamic enhancement factor of CEB model proposed by EIBL (1988)

$$\frac{f_{td}}{f_t} = \left(\frac{\dot{\varepsilon}}{\dot{\varepsilon_0}}\right)^{1.016\delta} \quad \dot{\varepsilon} \leq 30 s^{-1} \tag{5}$$

$$\delta = \frac{1}{10 + f_{cu}/2} \tag{6}$$

here, the quasi-static strain rate of concrete tensile strength is $\dot{\varepsilon_0}$=3.0× 10^{-6}s-1.

3. Modal analysis

Modal analysis has been conducted on the structure, and the results for the first eight modes of the bridge model are presented in Fig. 4. The fundamental frequency of the bridge is 0.1967 Hz. The first mode exhibits asymmetric vertical bending of the main beam.

4. Selection of seismic waves

The spatial effect of ground motion is primarily represented by the amplitude and phase relationship among its components or supporting points. Considering both phase and amplitude variations, these relationships are expressed in Eqs. (9) and (10)

$$a_1(t) = Ca_2(1 + t) \qquad C \leq 1 \tag{9}$$

$$A_1(w) = C(w) A_2(w)^{ip\omega} \tag{10}$$

In these equations, $C(w)$ represents the attenuation coefficient of amplitude, which indicates the attenuation is frequency-dependent; pw represents the phase difference of the frequency component, and Ai represents the amplitude.

Taking the El Centro earthquake wave with a peak acceleration of 0.3 g as an example, six sets of ground motion time histories have been calculated. The time history curves for the ground motion in both the longitudinal and vertical directions at the pier bases of #2, #3, and #4 are depicted in

Fig. 5.

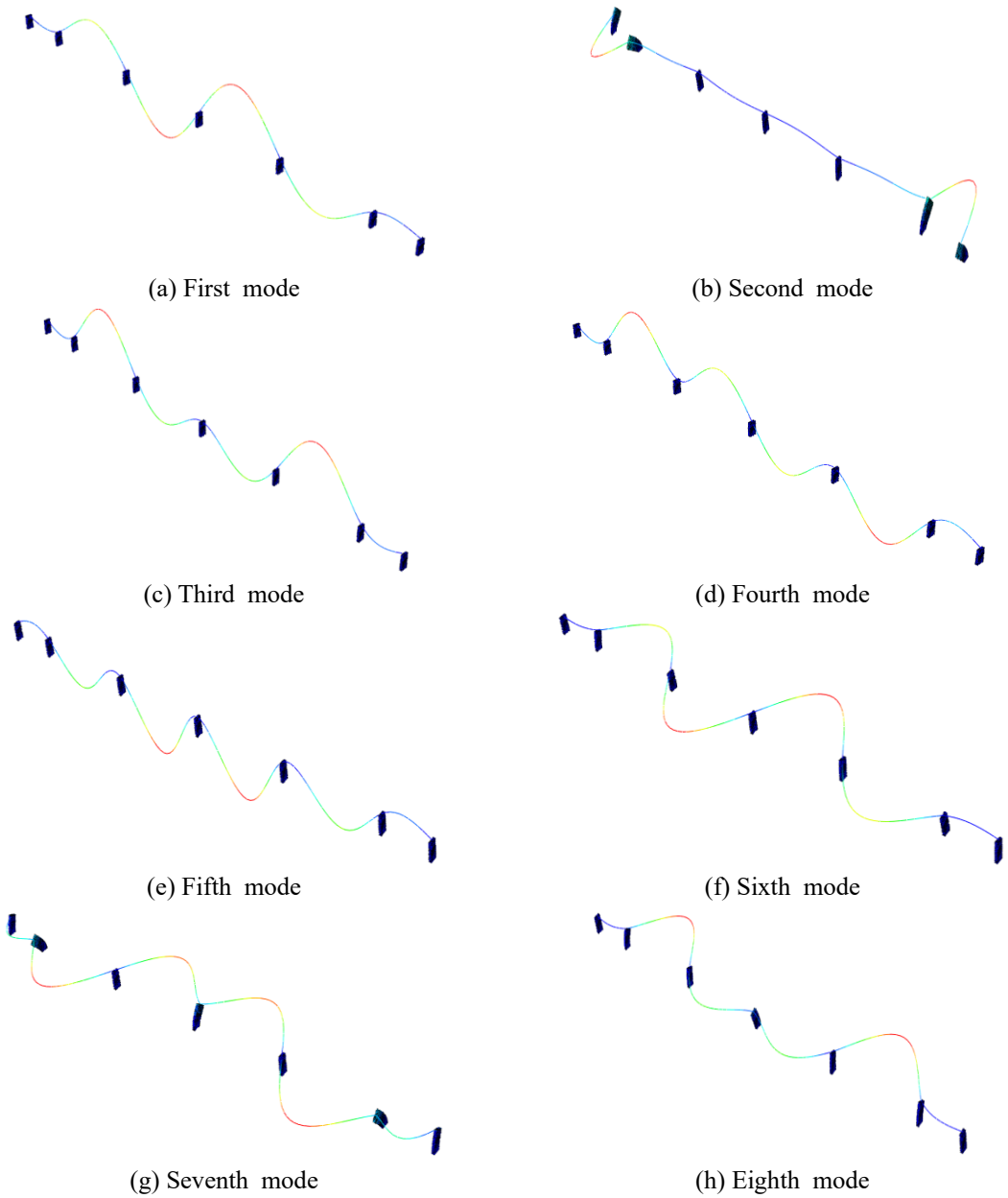

(a) First mode (b) Second mode

(c) Third mode (d) Fourth mode

(e) Fifth mode (f) Sixth mode

(g) Seventh mode (h) Eighth mode

Fig. 4 Diagrams of the first eight modes

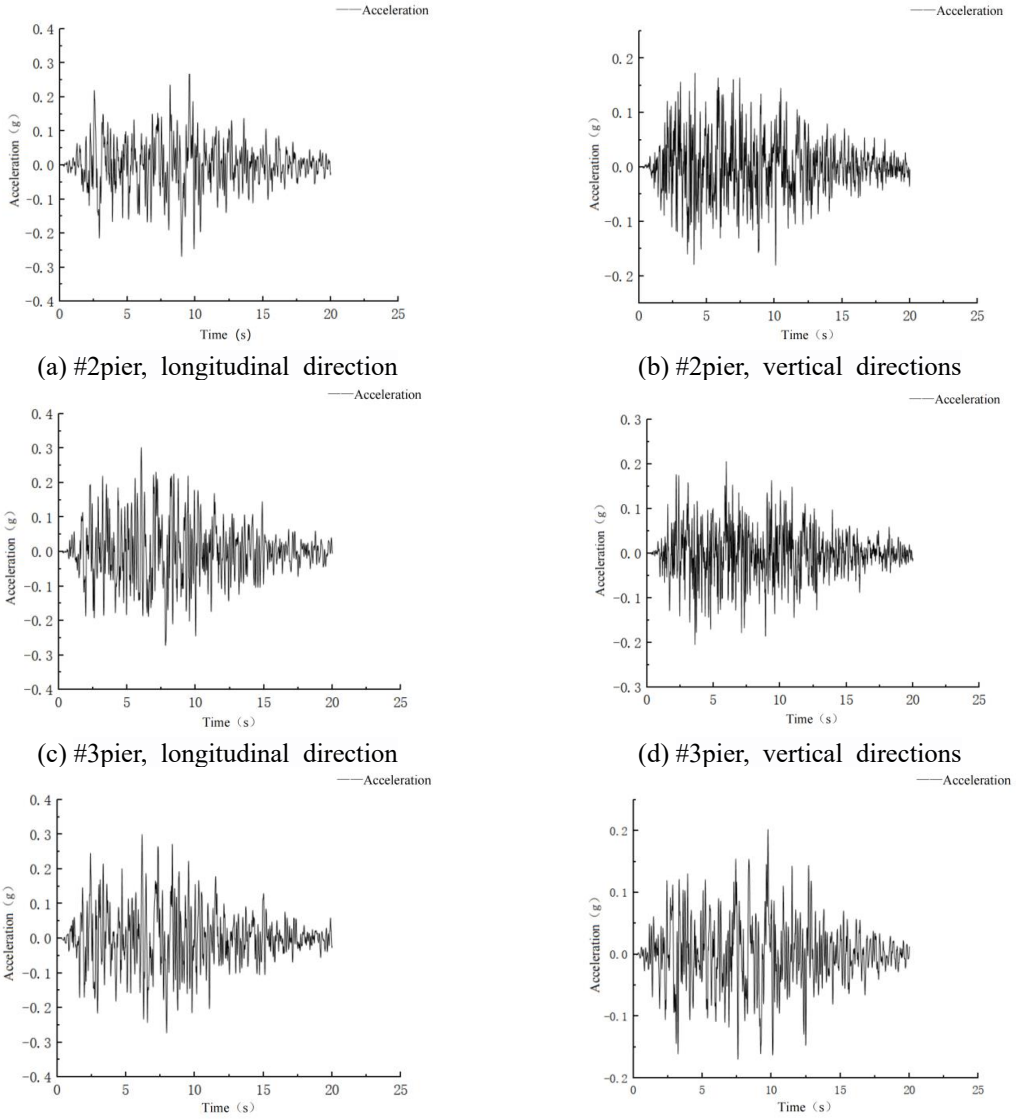

(a) #2pier, longitudinal direction (b) #2pier, vertical directions

(c) #3pier, longitudinal direction (d) #3pier, vertical directions

(e) #4pier, longitudinal direction (f) #4pier, vertical directions

Fig. 5 Ground motion time-history curve

5. Analysis of calculation results

5.1 Pier-top displacements

Taking the El Centro wave as an illustrative example, when the maximum acceleration amplitude reaches 0.3 g, considering the strain rate effect of the material, the time-history curves of the pier-top displacements in the longitudinal direction of piers #1 to #4 under multi-support excitation and uniform excitation are shown in Fig. 6; Conversely, under the same conditions but

Table 2 Top displacements of piers (m)

Strain rate	Multi-support excitation	#1	#2	#3	#4	#5	#6	#7
Yes	No	0.0238 (-34.3%)	0.0238 (-36.4%)	0.0267 (-27.6%)	0.0284 (-31.9%)	0.0267 (-27.6%)	0.0238 (-36.4%)	0.0238 (-34.3%)
Yes	Yes	0.0227 (-37.3%)	0.0374 0	0.0424 (14.9%)	0.0330 (-20.9%)	0.0384 (4%)	0.0339 -(9.4%)	0.0314 (-13.3%)
No	No	0.0362 (0)	0.0374 (0)	0.0369 (0)	0.0417 (0)	0.0369 (0)	0.0374 (0)	0.0362 (0)
No	Yes	0.0376 (3.9%)	0.0428 (14.4%)	0.0530 (43.6%)	0.0423 (1.4%)	0.0430 (16.5%)	0.0457 (22.2%)	0.0376 (3.9%)

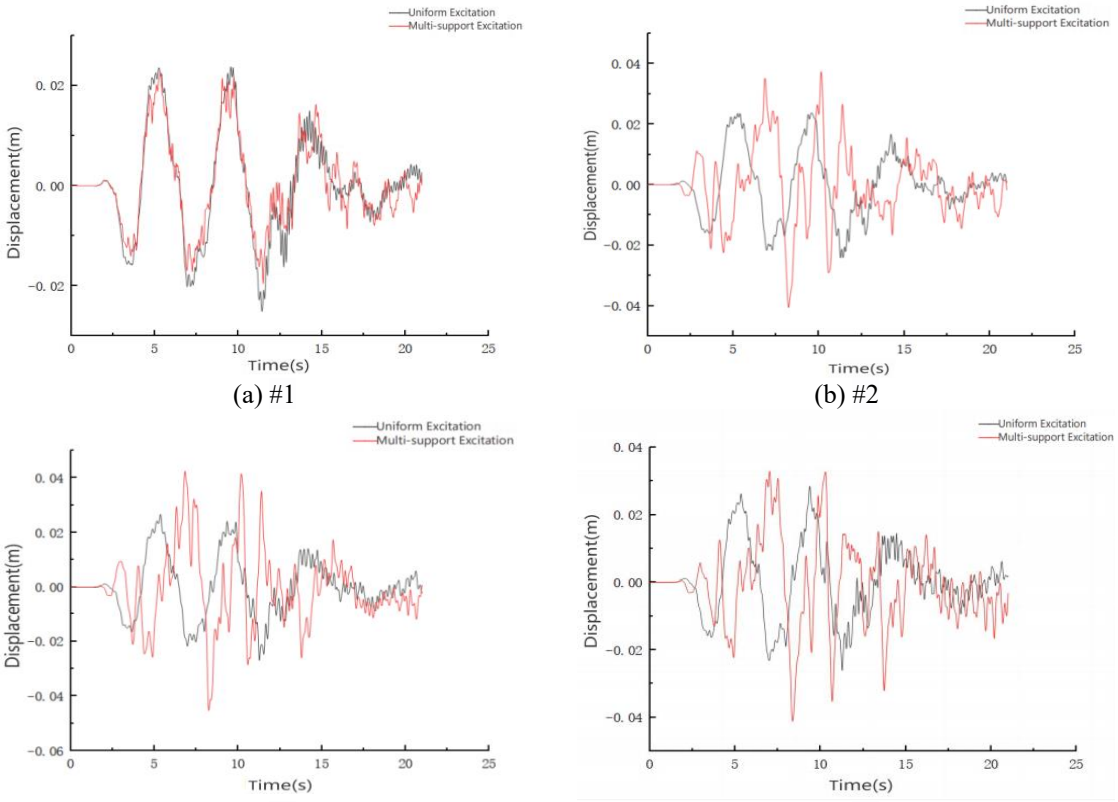

(a) #1 (b) #2

(c) #3 (d) #4

Fig. 5 Ground motion time-history curve

without considering the strain rate effect, the corresponding time-history curves for the pier-top displacements in the longitudinal direction are shown in Fig. 7. The peak displacement values at the top of each pier under the El Centro wave excitation for various conditions are listed in Table 2. The values enclosed in parentheses indicate the percent increase of top displacement compared to the case where neither the strain rate effect nor multi-point excitation are considered.

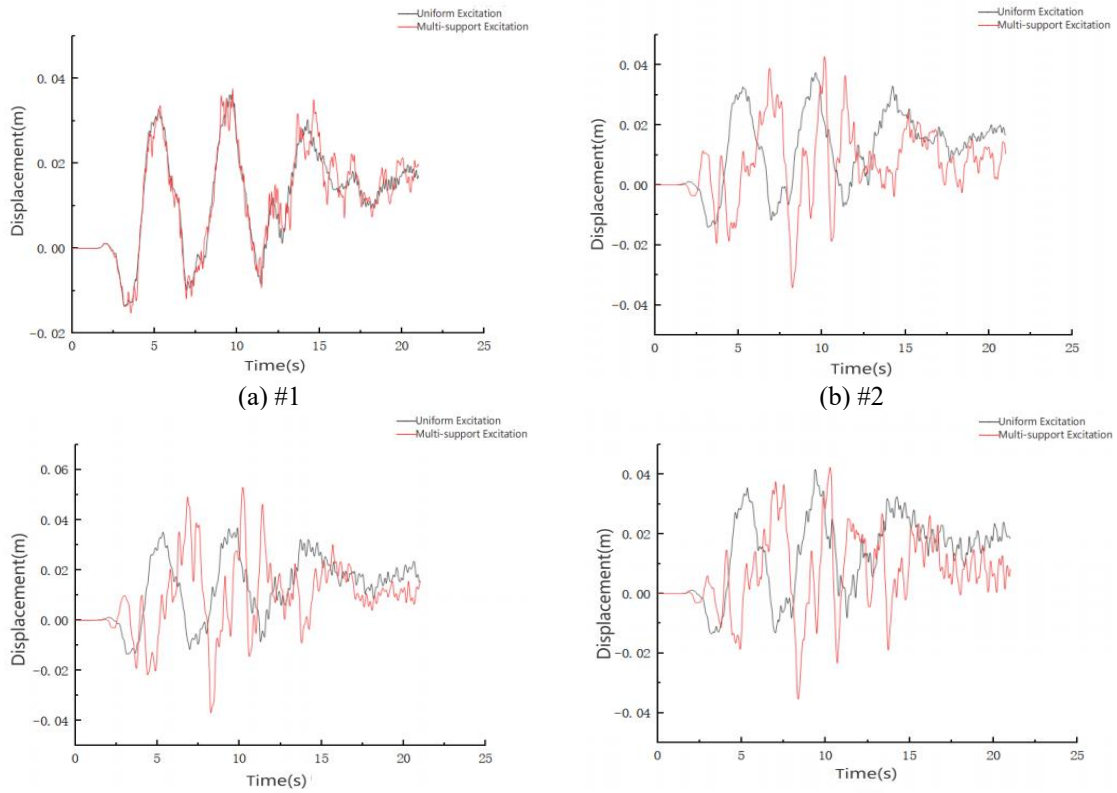

Fig. 7 Time-history curves of pier-top displacement without considering the strain rate effect

From Figs. 6 and 7, it can be observed that the peak displacements of the pier under multi-point excitation are higher compared to those under uniform excitation, irrespective of whether the strain rate effect of the material is taken into account. For instance, when the strain rate effect of the material is neglected, the peak displacement at the top of Pier #3 under uniform excitation is 0.0369 m, whereas under multi-point excitation, it increases to 0.053 m, marking a 43.6% rise. When the strain rate effect is considered, the peak displacement at the top of Pier #3 under uniform excitation is 0.0267 m, and under multi-point excitation, it rises to 0.0424 m, indicating a 58.8% increase. This indicates that, due to the spatial effect of seismic motion, the pier-top displacement of the bridge will increase regardless of whether the strain rate effect of the material is factored in.

As can be seen from Table 2, the pier top displacements of the bridge decrease when the rate-dependent effects of the material is considered only, the pier top displacements increase When the spatial effect of ground motion is considered only. For instance, the peak displacement at the top of pier #3 is 0.0369 m when neither the strain-dependent effects nor the spatial effects are considered. The value decreases to 0.0267 m when only the strain-dependent effects are considered. However, when only the spatial effects are considered, the displacement increases to 0.0530 m. The displacement is 0.0424 m when both the strain-dependent effects and the spatial effects are considered . This shows that the rate-dependent effects of the material can partly offset the impact of the spatial effects of seismic ground motion on the bridge displacement.

5.2 Base shear force of pier

Under the excitation of El Centro wave, the time-history curves of the pier base shear force along the bridge direction for each pier are depicted in Figs. 8 and 9. The peak shear force values at the base of each pier under different working conditions are presented in Table 3.The values enclosed in parentheses indicate the percent increase of shear value relative to the case where neither strain rate nor multi-point excitation are considered.

From Figs. 8 and 9 and Table 3, it can be seen that, the peak shear forces of the pier under multi-point excitation exhibit increase compared to uniform excitation, regardless of whether the strain rate effects of the material are considered.When only the strain rate effect of the material is taken into account, the peak shear force of pier #6 increases by 23.8%. When only the spatial effects(multi-point excitation) are considered, the peak shear force of pier #6 increases by 48.9%. When both the strain-dependent effects and the spatial effects are considered, the peak shear force of pier #6 increases by 59.4%. These results indicate that the response of the pier shear force is more intense under multi-point excitation, considering the effects of strain rate of material.

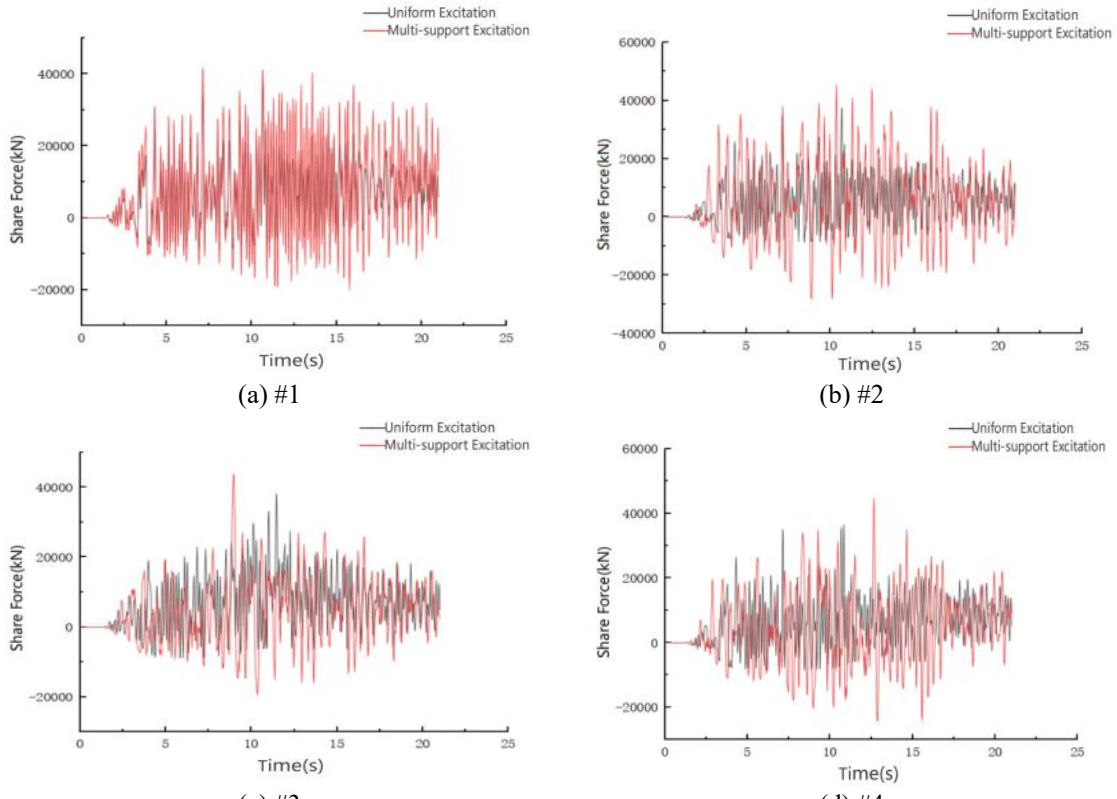

Fig. 8 Time history curve of shear force at pier base considering the strain rate effect

Table 3 The peak shear force at the base of each piers (kN)

Strain rate	Multi-support excitation	#1	#2	#3	#4	#5	#6	#7
Yes	No	38491 (2.9%)	36157 (-3.6%)	38456 (1%)	36321 (0.5%)	38466 (1%)	35469 (23.8%)	39502 (15.6%)
Yes	Yes	41654 (11.3%)	45394 (21%)	43778 (15%)	44772 (22.7%)	44658 (17.3%)	45682 (59.4%)	43325 (26.7%)
No	No	37415 (0)	37524 (0)	38059 (0)	36488 (0)	38085 (0)	28655 (0)	34187 (0)
No	Yes	38409 (2.7%)	41152 (9.7%)	43980 (15.6%)	40831 (11.9%)	41594 (9.2%)	42658 (48.9%)	40336 (18%)

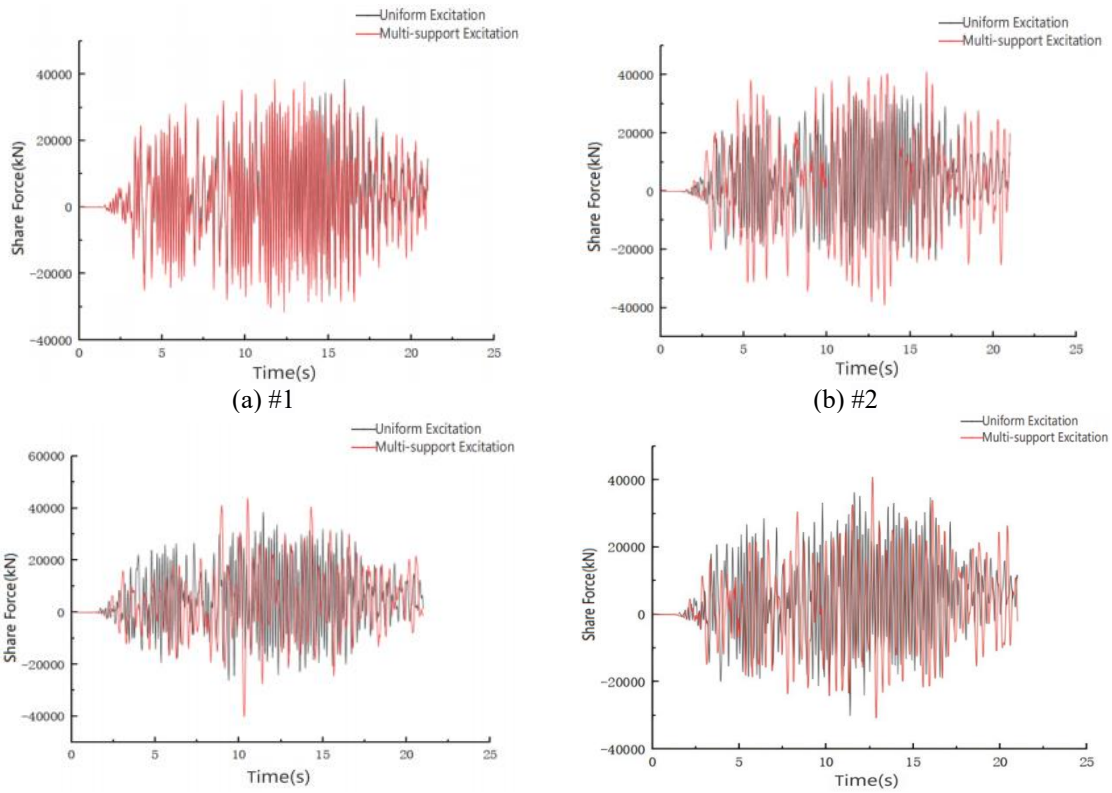

(a) #1 (b) #2

(c) #3 (d) #4

Fig. 9 Time history curve of shear force at pier base without considering the strain rate effect

6. Conclusions

This paper investigates the influence of material strain rate on the spatial effects of seismic excitation on bridge. The study primarily considers the factors such as strain rate and spatial nature of seismic. Utilizing the ABAQUS finite element software, a bridge model is established, and the time-history analysis method is employed to simulate the dynamic responses of the bridge under

seismic loads. Taking the El Centro wave as an example, the pier-top displacements and pier-base shear forces of the bridge are calculated, and the displacement time-history curves and shear force time-history curves are plotted, and the following conclusions are gotten.

- Regardless of whether the spatial effects of seismic excitation are considered, the strain rate effect of materials reduces the pier-top displacement of the bridge and increases the pier-base shear force.
- Irrespective of whether the material rate-dependency effects are considered, the spatial effects of seismic excitation increase both the pier-top displacement and the pier-base shear force .
- The strain rate effects of materials weaken the impact of seismic spatial effects on the pier displacement of the bridge to a certain degree.

When analyzing the seismic response of bridges, considering both the strain rate effects of materials and the spatial effects of seismic excitation enables more accurate predictions of the bridge's behavior under earthquake conditions.

Acknowledgments

This work was financially supported by the Science Foundation of Liaoning Provincial Department of Education (LJKZ0720).

References

Chen, L., Fang, Q., Zhang Y. and Zhang, Y. (2008), "Rate-sensitive numerical analysis of dynamic responses of arched blast doors subjected to blast loading", *Transactions of Tianjin University*, **2008**(14), 348-352. https://doi.org/10.1007/s12209-008-0059-x.

Chen, X., Chen, C., Liu, Z., Lu, J. and Fan, X. (2018), "Compressive behavior of concrete under high strain rates after freeze-thaw cycles", *Comput. Concrete*, **21**(2), 209-217.

EIBL J. (1988), "Concrete structures under impact and impulsive loading (CEB-Bulletin d'information, NO.187)", Comite Euro-International du Beton, Dubrovnik.

Fu, H.C., Erki, M.A. and Seckin, M. (1991), "Review of effects of loading rate on reinforced concrete", *J. Struct. Eng.*, **117**(12), 3660-3679.

Fujikake, K., Mori, K., Uebayashi K., Ohno, T. and Mizuncr, J. (2000), "Dynamic properties of concrete materials with high rates of tri-axial compressive loads", *Struct. Mater.*, **2000**(8), 511-522.

Gang H.G. and Kwak H.G.(2017),A tensile criterion to minimize FE mesh-dependency in concrete beams under blast loading. *Computers and Concrete,* 20(1)*,* 1-10.

JTG (2015), *General Specifications for Design of Highway Bridges and Culverts*, JTG D60, China.

Kim, S., Park, C. and Dong, J.M. (2020), "Dynamic tensile behavior of SIFRCCs at high strain rates", *Comput. Concrete*, **26**(3), 275-283. https://doi.org/10.12989/cac.2020.26.3.275.

Li, M. (2011), "Effects of rate-dependent properties of material on dynamic properties of reinforced concrete structural", Ph.D. Dissertation, Dalian University of Technology, Dalian.

Li, Z. (2010), "Constitutive model of concrete damage and earthquake damage analysis of reinforced concrete bridge under complex stress conditions", Ph.D. Dissertation, Tianjin University, Tianjin.

Liu, G.H., Xinzheng, L. and Wei, G. (2014), "Study on steel strain-rate and multiple earthquake motions effect on elasto-plasticity responses of 300 m span single tower cable-stayed bridge", *Chinese J. Comput. Mech.*, **2014**(4). https://doi.org/486-493.10.7511/jslx201404012.

Liu, J.C., Fang, Q., Gong, Z.M., *et al*. (2003), "Analysis of the dynamic response and failure form of reinforced concrete beam under the action of explosion load", *Explosion and Impact*, **23**(1), 25-30.

Liu, Y. (2019), "Dynamic response of offshore bridges under seabed ground motions", M.S. Dissertation, Dalian Jiaotong University, Dalian.

Nam, J.W., Yoon, I.S. and Yi, S.T. (2016),"Numerical evaluation of FRP composite retrofitted reinforced concrete wall subjected to blast load", *Comput. Concrete*, **17**(2), 215-225. https://doi.org/10.12989/cac.2016.17.2.215.

Nie, L.X., Xu, J.Y. and Bai, E. (2017) "The research on static and dynamic mechanical properties of concrete under the environment of sulfate ion and chlorine ion", *Comput. Concrete*, **20**(2), 205-214. https://doi.org/10.12989/cac.2017.20.2.205.

Pang, Z.H. (2009), "Research on the treatment method for bottom crack failure of prestressed continuous rigid frame bridges", Ph.D. Dissertation, Chang'an University, Chang'an.

Suaris, W. and Shah, S.P. (1983), "Properties of concrete subjected to impact", *J. Struct. Eng.*, **109**(7), 1727-1741.

Takeda, J., Tachikawa, H. and Fujimoto, K. (1974), "Mechanical behavior of concrete under higher rate loading than in static test", *Mech. Behav. Mater.*, **1974**(2), 479-486.

Wei, J., Quintero, R. Galati, N. and Nanni, A. (2007), "Failure modeling of bridge components subjected to blast loading. part1: Strain rate-dependent damage model for concrete", *Int. J. Concrete Struct. Mater.*, **1**(1), 19-28. https://doi.org/10.4334/IJCSM.2007.1.1.019.

Yan, S., Zhang, L. and Wang, D. (2005), "Analysis of the failure pattern of reinforced concrete slab under the explosion load", *J. Shenyang Jianzhu Univ.*, **21**(3), 177-180.

Yu, W.J., Shi, J.Y. and Zhao, J.C. (2011), "Research on the dynamic mechanical properties of Q345 steel products", *Build. Struct.*, **41**(3), 28-30. https://doi.org/28-30.10.19701/j.jzjg.2011.03.007.